Electronic Supplementary Material (ESI) for Journal of Materials Chemistry A.

Electronic Supplementary Information

Multicomponent Transition Metal Phosphides Derived from Layered Double Hydroxide Double-Shelled Nanocages as an Efficient Non-precious Co-catalyst for Hydrogen Production

D. Amaranatha Reddy, Hyun Kook Kim, Yujin Kim, Seunghee Lee, Jiha Choi, M. Jahurul Islam, D. Praveen Kumar and Tae Kyu Kim*

Department of Chemistry and Chemical Institute for Functional Materials, Pusan National University, Busan 609-735, Republic of Korea

*E-mail: tkkim@pusan.ac.kr

1. EXPERIMENTAL SECTION

1.1 Synthesis of Zeolitic imidazolate framework-67 (ZIF-67) rhombic dodecahedrons

Uniform sized ZIF-67 rhombic dodecahedrons were synthesized by a facile solution approach. In a typical synthesis process aqueous methanolic solutions of cobalt nitrate hexahydrate (4 mmol, 50 ml) and 2-methylimidazole (8 mmol, 50 ml) were prepared separately, and then solutions were mixed with strong magnetic stirring at room temperature. When the two solutions were mixed together stirring was stopped and aged for 24 h. At last, the purple precipitate was collected by centrifugation, washed with ethanol, methanol and then finally dried at 60 °C for 10 h to obtain the final products.

1.2 Synthesis of yolk-shelled ZIF-67@ layered double hydroxides (LDH)

To synthesize ZIF-67@LDH, the above synthesized ZIF-67 (40 mg) was first dispersed in 20 mL of ethanol. Then, required stoichiometry amount of ethanolic solution of Ni(NO3)2·6H2O (90 mg) quickly poured into the former purple dispersion. The mixture was vigorously stirred for 30 min to obtain a homogeneous suspension. After completion of the reaction, the final products were collected and washed several times with ethanol to remove the impurities and finally heated in air at 80 °C for 10 h to obtain the final products.

1.3 Synthesis of Double-shelled cobalt hydroxide and layered double hydroxides Nanocages (CH@LDH)

To synthesize CH@LDH, the above synthesized ZIF-67@LDH nanostructures (40 mg) were dispersed in 20 mL of ethanol and then 50 mg of Na_2MoO_4•$2H_2O$ DI-water solution was quickly poured into the former dispersion under stirring. Then, this suspension was maintained at 85 °C until the purple color disappeared entirely. After completion of the reaction, the solution was air

cooled to room temperature. Finally the products were collected and washed several times with DI water to remove the impurities and finally heated in air at 80 °C for 10 h to obtain the final products.

1.4 Synthesis of Multi component transition Metal phosphides (*MCTMPs)*

For MCTMPs synthesis the above synthesized CH@LDH nanostructures (50 mg) and 250 mg of NaH2PO2 were mixed thoroughly and placed in a alumina crucible in a closed system and heated at 300 ^{o}C for 1h with a heating rate of 2 ^{o}C/min. Finally obtained black solid was washed subsequently by water and ethanol three times to get the final products. Similar synthesis procedure was applied for the synthesis of ZIF-67-MPs, LDH-MPs.

1.5 Synthesis of CdS nanorods

CdS nanorods were synthesized via a hydrothermal method. A typical synthetic process involved dissolving $Cd(CH_3COO)_2{\cdot}2H_2O$ (3.2 mmol), CH_4N_2S (16 mmol) at the required stoichiometry into 60 mL ethylenediamine. After stirring for 2 h, the solution was transformed to 80 ml Teflon-lined autoclave and was placed inside a furnace and heated at 160 °C for 48 h. After completion of the reaction, the autoclave was air-cooled to room temperature. The products were collected and washed several times with DI water to remove any impurities and then finally heated in air at 100 °C for 6 h to obtain the final products.

1.6 Synthesis of CdS/MCTMPs nanocomposites

To synthesize CdS/MCTMPs nanocomposites, the synthesized CdS and desired wt.% of MCTMPs (1, 2, 3, 4 and 5) were dispersed in 20 mL of ethanol in a separate beaker and both of the samples were sonicated for 30 minutes. After sonication, MCTMPs suspension was mixed with the CdS solution. The mixture was vigorously stirred for 12 h to obtain a homogeneous suspension. After

completion of the reaction, the products were collected and washed several times with DI water to remove the impurities and finally heated in air at 100 °C for 6 h to obtain the final products. CdS-MCTMPs with different MCTMPs contents was prepared following the same method with different wt.% of MCTMPs as the reactant. Similar synthesis procedure was applied for the synthesis of CdS/ZIF-67-MPs, CdS/LDH-MPs.

2. Characterization

The morphologies and average particle sizes were measured using a Hitachi S-4800 field emission scanning electron microscope (FESEM) equipped with an Inca 400 energy-dispersive spectrometer from Oxford Instruments. The microstructure properties were measured using a JEOL JEM-2100F transmission electron microscope (TEM) with an accelerating voltage of 200 kV. Phase determination of the as-prepared powders was performed using a Bruker D8 Advance X-ray diffractometer with a Cu Kα X-ray source. X-ray photoelectron spectroscopy (XPS) was performed using a monochromated Al Kα X-ray source (hν = 1486.6 eV) at an energy of 15 kV/150 W. The nitrogen adsorption–desorption isotherm measurements for the samples were carried out at 77.35 K using a Tristar 3000 Micromeritics instrument to measure the surface area. The optical absorption measurements were performed using a Shimadzu UV-1800 double-beam spectrophotometer. Photoluminescence (PL) measurements were performed at room temperature using Hitachi F-7000 fluorescence spectrophotometer with an excitation wavelength of 380 nm.

2.1 Photocatalytic hydrogen Production

The photocatalytic hydrogen evolution experiments were performed in a Pyrex flask (containing 12 ml of DI-water, 3 ml of lactic acid as sacrificial agent and 1 mg of photo-catalyst) at ambient temperature and atmospheric pressure. The openings of the flask were sealed with

silicone rubber septum. A solar simulator equipped with an AM 1.5G filter and 150 W Xe lamp (Abet Technologies) was used as the light source. The output light intensity was adjusted to 1 sun (100 W/m^2) using 15151 low-cost calibrated Si reference cell (ABET technologies). Before irradiation, the system was evacuation and bubbled with Ar for 30 min to remove the air inside. The hydrogen gas evolved was determined using an off-line gas chromatograph (Young Lin Autochro-3000, model 4900) equipped with thermal conductivity detector.

The apparent quantum efficiency (QE) was measured according to the equation below

$$QE = \frac{\text{nuber of reacted electrons}}{number\ of\ incident\ photons} \text{ x } 100\ \%$$

$$= \frac{\text{number of evolved } H_2 \text{molecules x } 2}{number\ of\ incident\ photons} \text{x} 100\%$$

Here the QE was measured under the same photocatalytic hydrogen evolution experimental conditions except the irradiation source, here 150 W Xe lamp with 425 nm band pass filter were used as light sources, instead of the solar simulator. The output light intensity was measured using 15151 low-cost calibrated Si reference cell (ABET technologies). The liquid level is ~16 cm far from the window of lamp and the illuminated area is 21.24 cm^2.

2.2 Photo-electrochemical measurements

Photo-electrochemical measurements were performed in a three-electrode system using a CHI 617B electrochemical workstation. A solar simulator equipped with an AM 1.5G filter and 150 W Xe lamp (Abet Technologies) was used as the irradiation source to produce monochromatic illuminating light. The output light intensity was adjusted to 1 sun (100 W/m^2) using 15151 low-cost calibrated Si reference cell (ABET technologies). The reference and counter electrodes were

Ag/AgCl and platinum wire, respectively, and Na_2SO_4 aqueous solution served as the electrolyte. To prepare the working electrode, the as-synthesized 10 mg of CdS and CdS/MCTMPs nanocomposites were first dispersed into ethanol (450 µl) and 50 µl Nafion mixtures using soft ultrasonic stirring to obtain a uniform suspension. The solution containing the catalyst (30 µl) was dropped onto the pretreated indium–tin oxide (ITO) conductor glass substrate, which was then dried in an oven at 100 °C for 3 h. Photo-responses were measured at 0.0 V during on-off cycling of the solar simulator. Electrochemical impedance spectroscopy (EIS) was carried out at open-circuit potential over the frequency range of 10^5 and 10^{-1} Hz with an AC voltage magnitude of 5 mV. Moreover, to evaluate the flat-band potential (V_{FB}) of the CdS and MCTMPs, Mott−Schottky plots at a frequency of 1 kHz were measured using a standard potentiostat equipped with an impedance spectra analyzer in the same electrochemical configuration and electrolyte under the dark condition. The measured potentials versus Ag/AgCl were converted to the normal hydrogen electrode (NHE) scale by $E_{NHE} = E_{Ag/Agcl} + 0.197$.

3. Supporting Figures

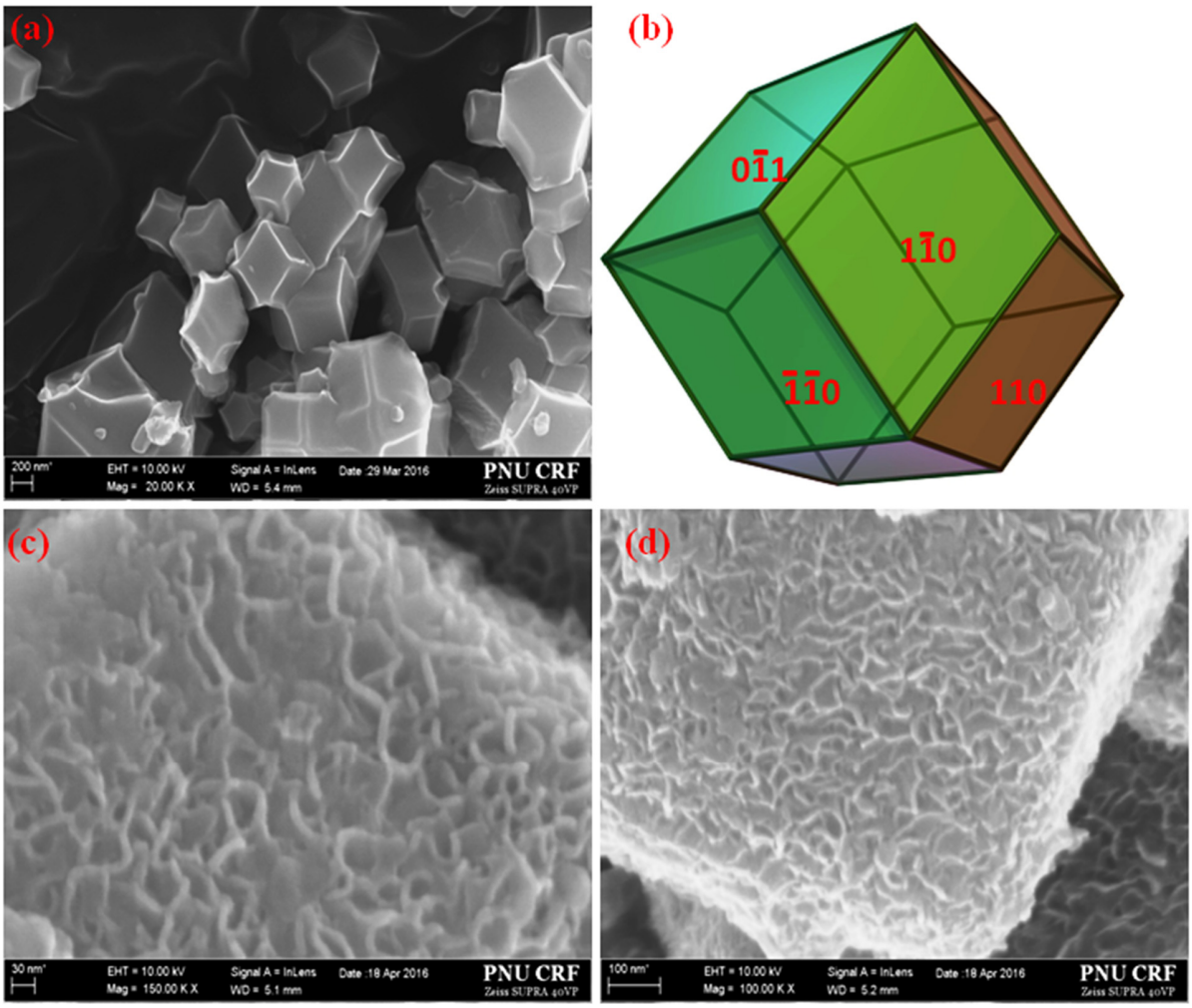

Figure S1. (a) High Magnification FESEM images of as-synthesized ZIF-67 product, (b) schematic illustration of the crystal orientation of the rhombic dodecahedral structure. (c, d) high magnification FESEM image of ZIF-67@LDH and CH@LDH respectively.

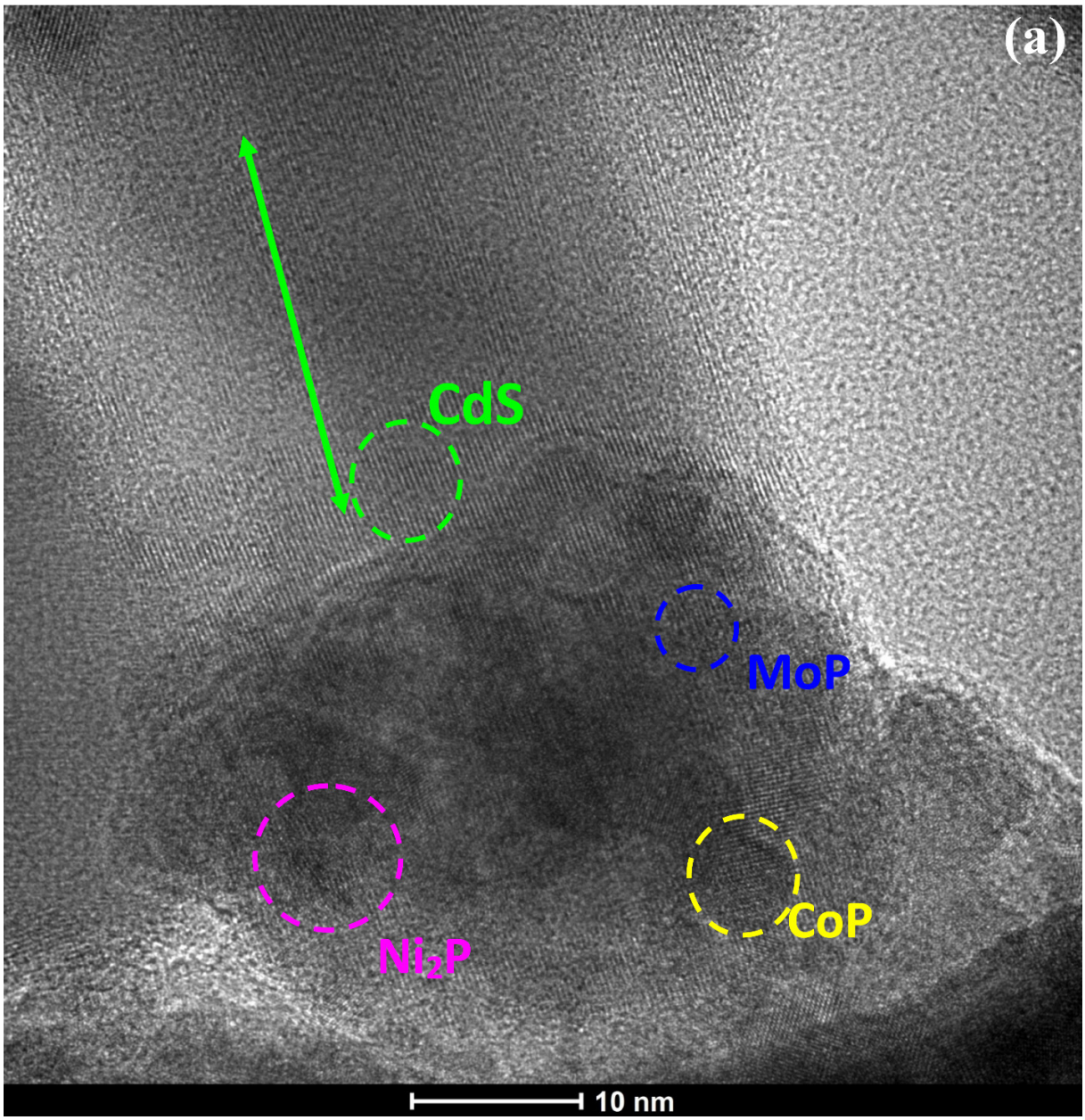
(a)
CdS
MoP
Ni2P
CoP
10 nm

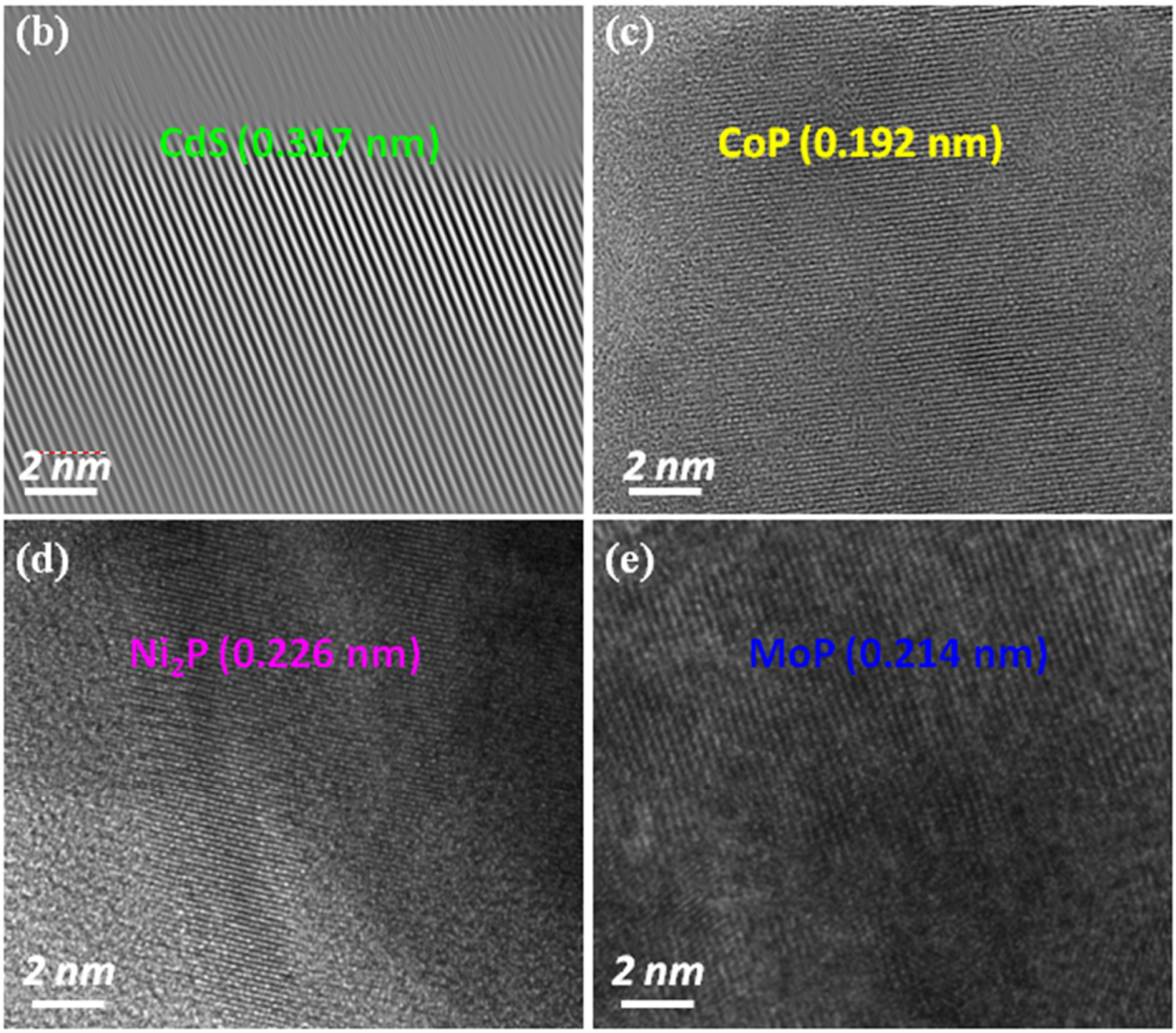

Figure S2. HRTEM images of (a) CdS/MCTMPs nanocomposite. (c) HRTEM image of corresponding CoP nanostructures in nanocomposite with interlayer spacing of 0.192 nm. (d) HRTEM image of corresponding Ni_2P nanostructures in nanocomposite with interlayer spacing of 0.226 nm. (e) MoP nanostructures with interlayer spacing of 0.214 nm.

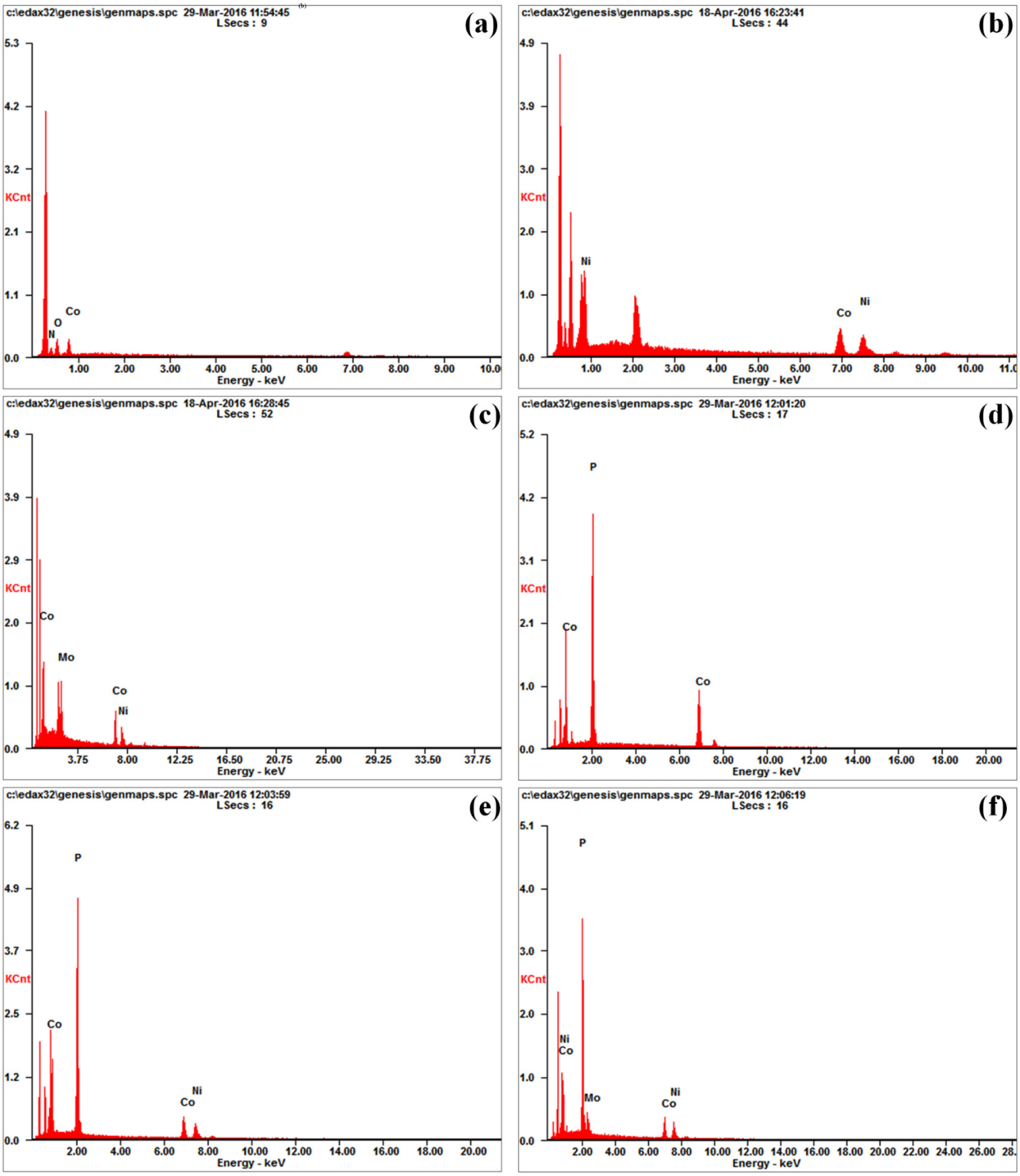

Figure S3. EDS spectra of (a) ZIF-67, (b) ZIF-67@LDH, (c) CH@LDH (d) ZIF-67-MPs (e) LDH-MPs (f) MCTMPs, respectively.

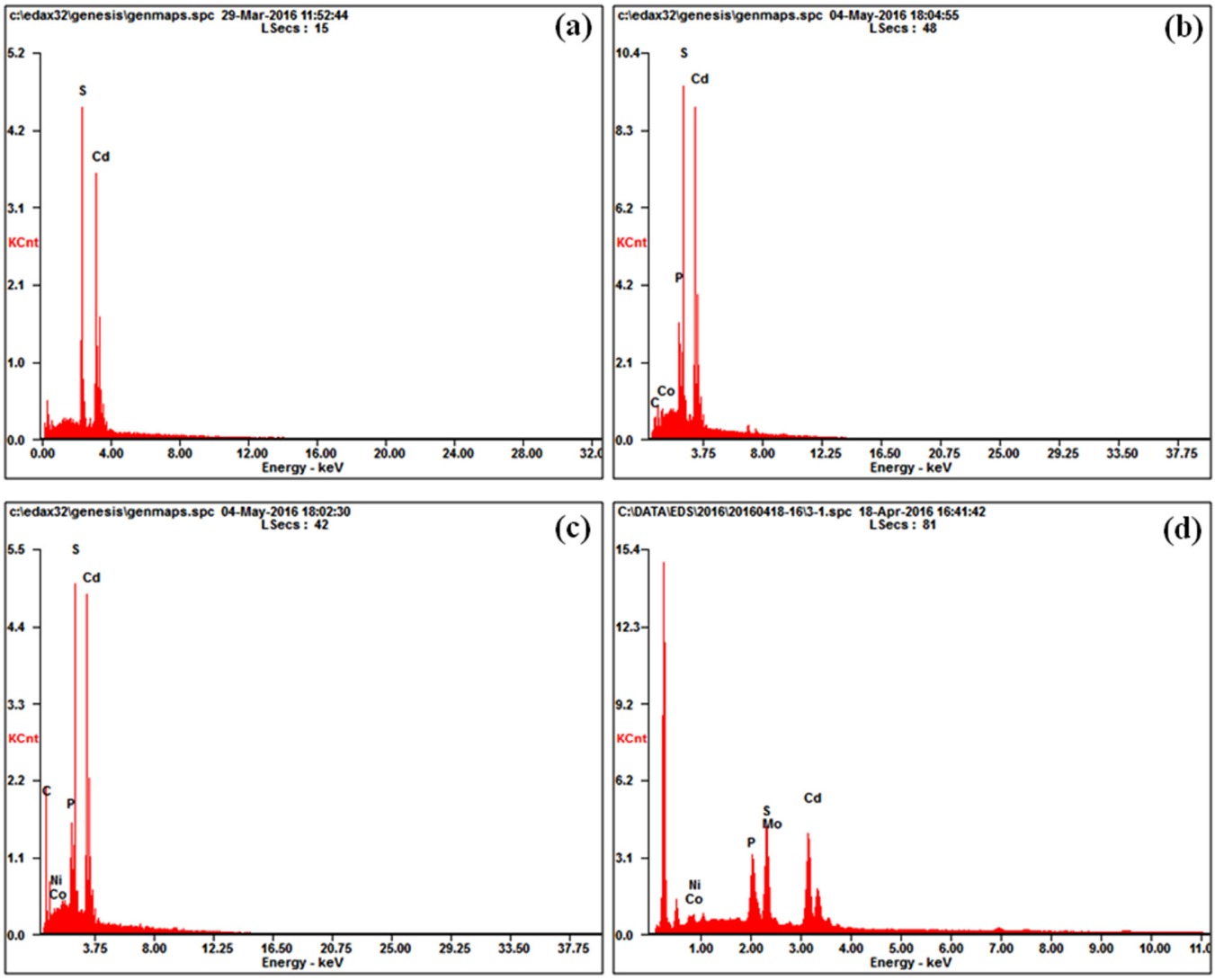

Figure S4. EDS spectra of (a) CdS, (b) CdS/ZIF-67-MPs (c) CdS/LDH-MPs (d) CdS/MCTMPs nanocomposites, respectively.

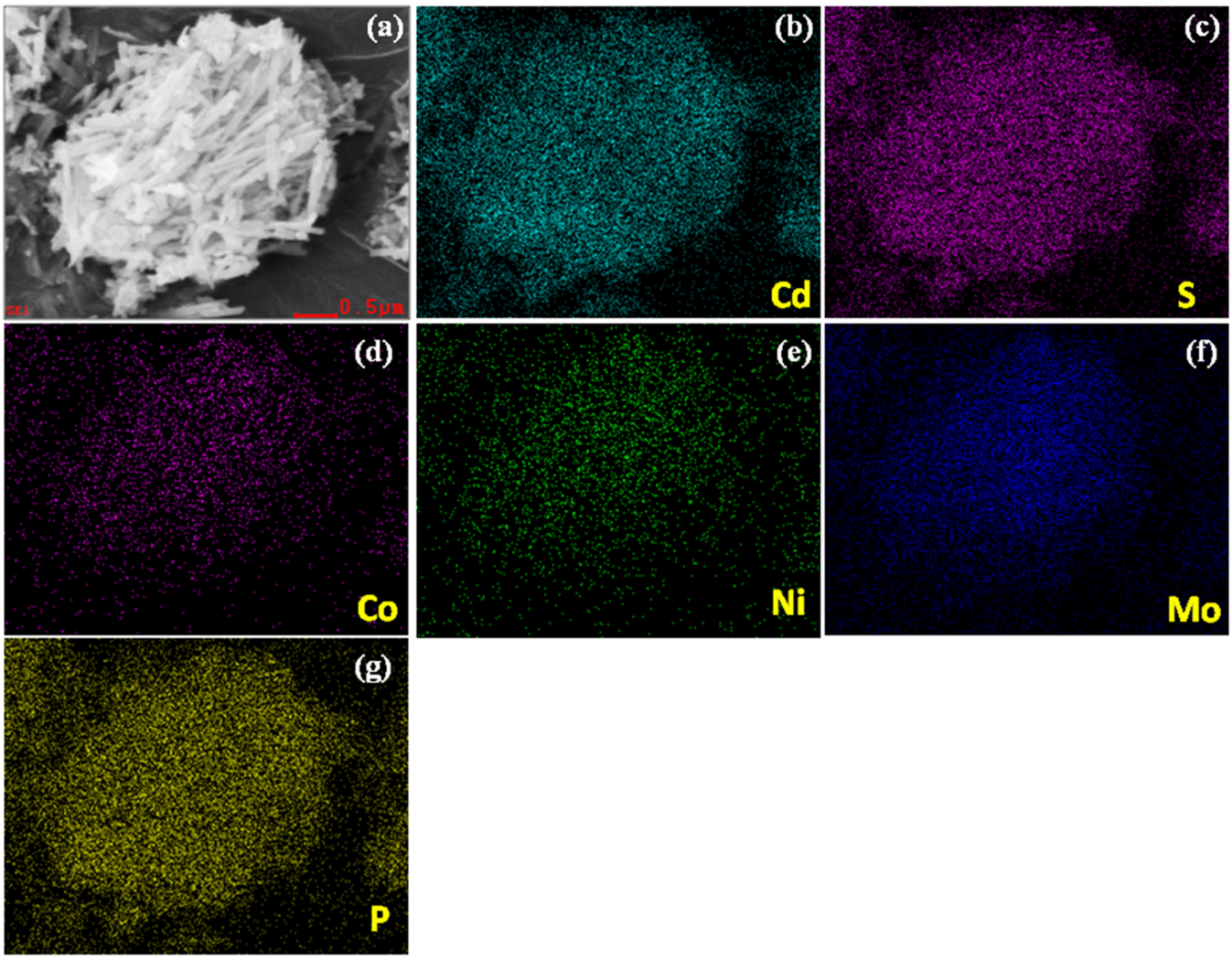

Figure S5. (a) FESEM electron micrograph and elemental mapping of CdS/MCTMPs (2 wt.%) nanocomposite showing the presence of (b) Cd (c) S (d) Co (e) Ni (f) Mo and (g) P elements, respectively.

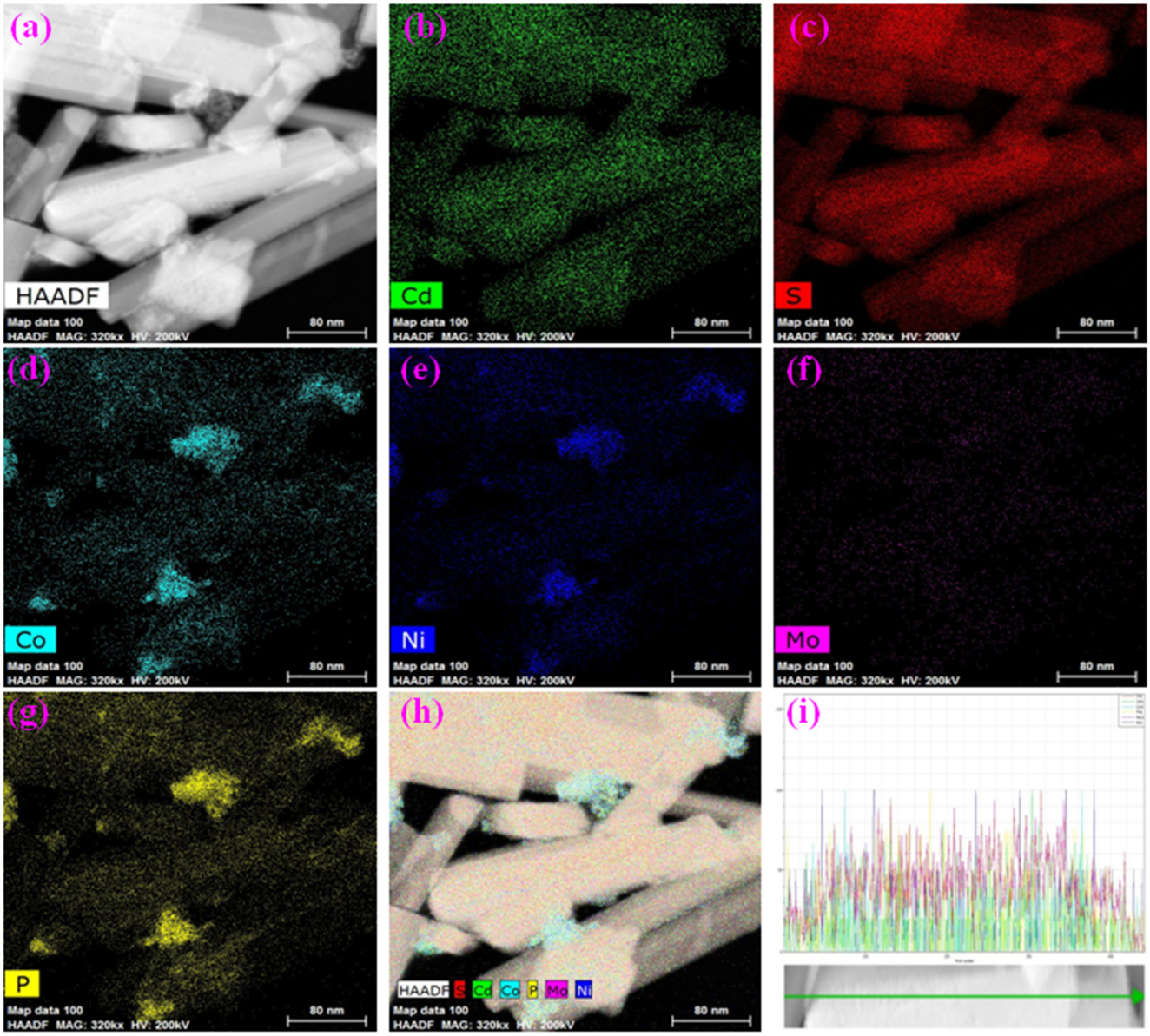

Figure S6. (a) TEM electron micrograph and elemental mapping of CdS/MCTMPs (2 wt.%) nanocomposite showing the presence of (b) Cd (c) S (d) Co (e) Ni (f) Mo (g) P (h) all elements and (i) line spectra of present elements, respectively.

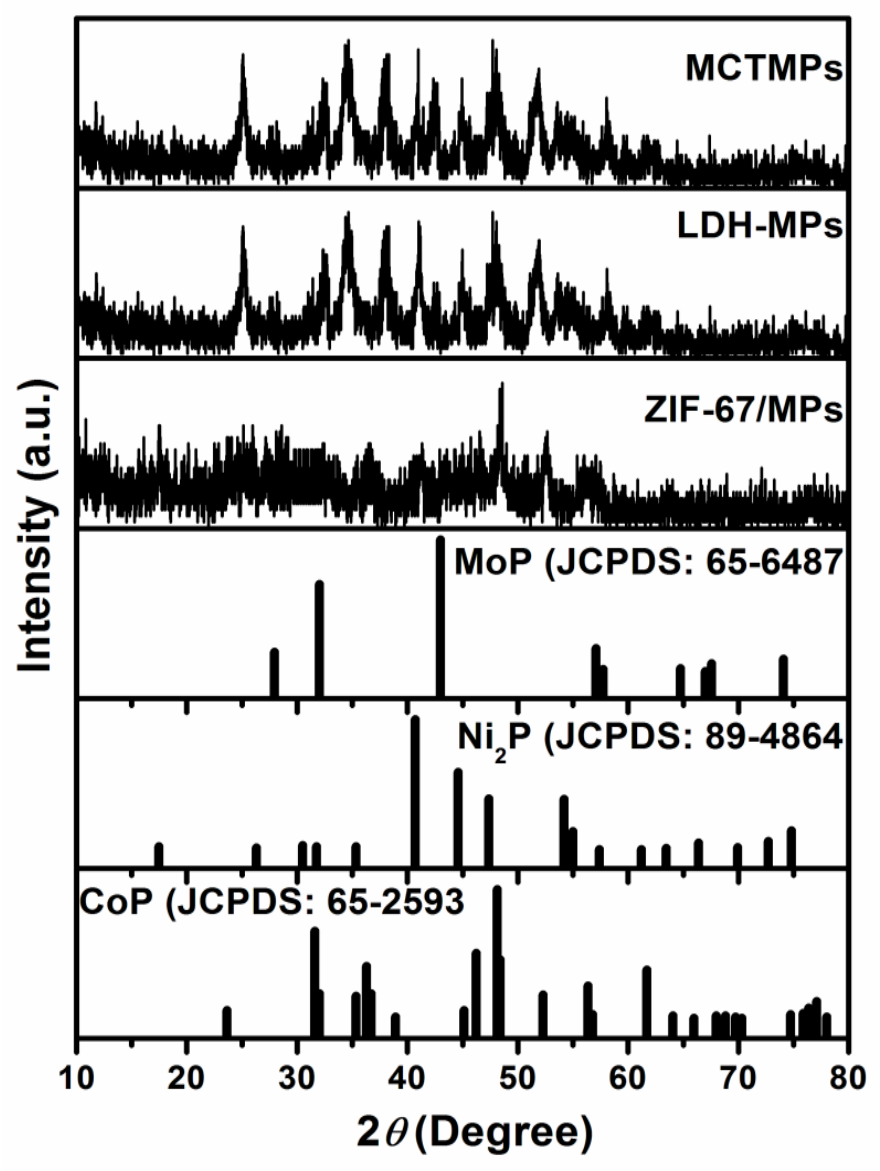

Figure S7. X-ray diffraction patterns of the ZIF-67-MPs, LDH-MPs, and MCTMPs nanostructures.

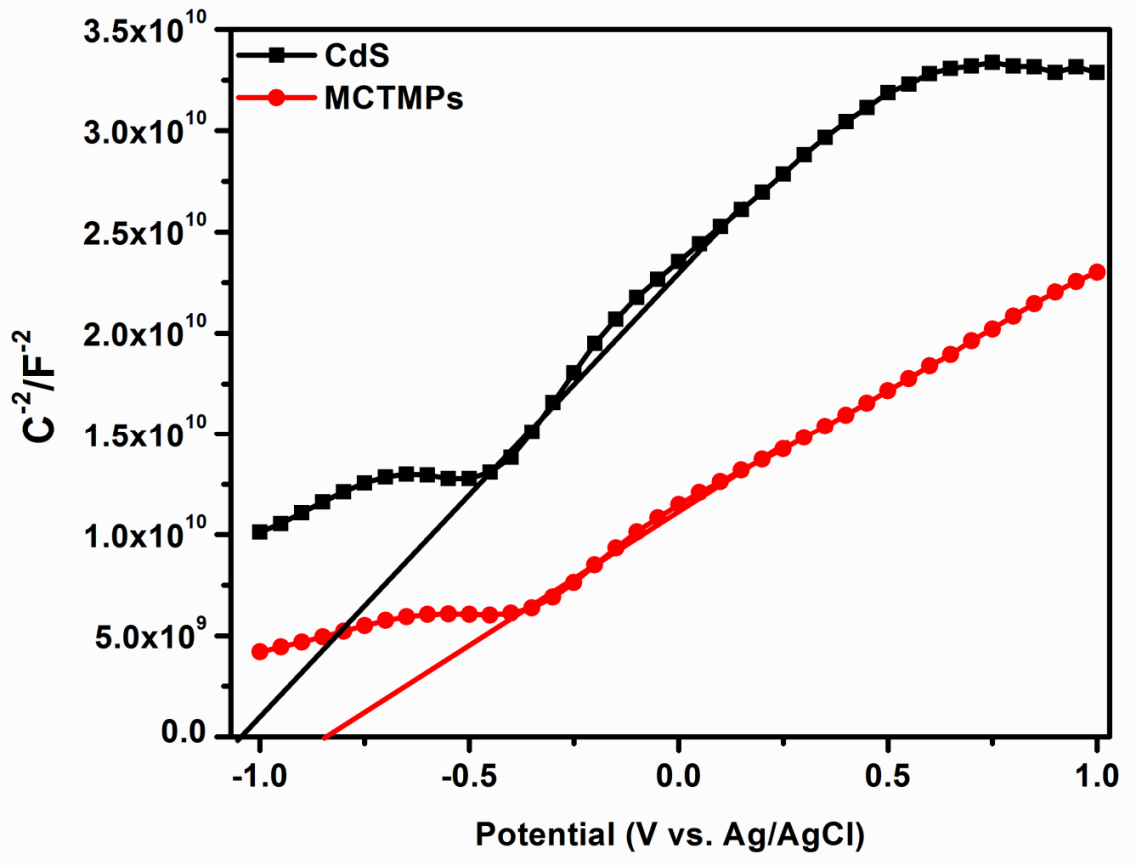

Figure S8. Mott-Schottky plots of CdS nanorods and MCTMPs nanostructures.

Table S1. Comparison of photocatalytic H_2 evolution rate reported in the literature using different co-catalysts on CdS nanostructures with our present results

Photocatalyst	Loading catalyst amount (mg)	Reported Hydrogen evolution Rate (μmol/mg/h)	Reported QE %	References
CdS/Co_2P	0.75	19.37	6.8	S1
CdS/Cu_3P	1	77.60	7.7	15
CdS/$Co(OH)_2$	50	14.43	6.09	S2
CdS/MoS_2	20	49.80	41.37	S3
CdS/BNNSs	50	0.439	0.73	S4
CdS-$Ni(OH)_2$/g-C_3N_4	1	115.18	16.70	S5
CdS@Au/U-WO_3	20	1.39	3.45	S6
CdS@Cd-Pt	100	1.21	33.0	19
CdS/CoP	20	106.0	27.1	S7
CdS/Co_3O_4	50	3.014	9.7	S8
CdS/C_3N_4-NiS	50	2.563	---	S9
CdS/Pt	50	33.0	56.3	S10
CdS/WS_2	10	1.984	---	S11
CdS/$Ni(OH)_2$	50	5.085	28	S12
CdS/Ni	--	63.0	53	S13
CdS/Ni(II)-Ti(IV)	50	3.437	--	S14
CdS/graphene/$ZnIn_2S_4$	100	1.94	56	S15
CdS/Ni_2P	1	553.7	41	12
CdS/Mo_2C	100	1.61	3.41	S16
CdS/RGO-MoS_2@CoP	1	83.907	22.5	13
CdS/Pd	50	16.28	---	S17
CdS/CoPx	1	500	35	S18
CdS/CeOx	50	1.290	---	S19
CdS/RGO-MoS_2	200	6.0	28.1	S20
PdS@CdS+$ZnS(en)_{0.5}$	40	2.6	23	S21
CdS/Ni-NiO/g-C_3N_4	100	12.587	----	S22
CdS/WS_2/graphene	8	1.842	21.2	S23
CdS/g-C_3N_4	50	4.152	4.3	S24
CdS/ Au/MIL-101	10	25	8.8	S25
CdS/MCTMPs	**1**	**136.77**	**40.6**	**Present Study**

References

[S1] S. Cao, Y. Chen, C. C. Hou, X. J. Lv, W. F. Fu, J. Mater. Chem. A, 2015, 3, 6096–6101.

[S2] X. Zhou, J. Jin, X. Zhu, J. Huang, J. Yu, W. Y. Wong, W.K. Wong, J. Mater. Chem. A, 2016, 4, 5282–5287.

[S3] X. L. Yin, L. L. Li, W. J. Jiang, Y. Zhang, X. Zhang, L. J. Wan, J. S. Hu, ACS Appl. Mater. Interfaces 2016, 8, 15258−15266.

[S4] F. Ma, G. Zhao, C. Li, T. Wang, Y. Wu, J. Lv, Y. Zhong, X. Hao, CrystEngComm, 2016, 18, 631–637.

[S5] Z. Yan, Z. Sun, X. Liu, H. Jia, P. Du, Nanoscale, 2016, 8, 4748–4756.

[S6] X. L. Yin, J. Liu, W. J. Jiang, X. Zhang, J. S. Hu, L. J. Wan, Chem. Commun., 2015, 51, 13842-13845.

[S7] D. Zhao, B. Sun, X. Li, L. Qin, S. Kang, D. Wang, RSC Adv., 2016, 6, 33120–33125.

[S8] D. Lang, F. Cheng, Q. Xiang, Catal. Sci. Technol. DOI: 10.1039/c6cy00753h.

[S9] J. Yuan, J. Wen, Y. Zhong, X. Li, Y. Fang, S. Zhang, W. Liu, J. Mater. Chem. A, 2015, 3, 18244–18255.

[S10] M. Luo, W. Yao, C. Huang, Q. Wu, Q. Xu, J. Mater. Chem. A, 2015, 3, 13884–13891.

[S11] J. Chen, X. J. Wu, L. Yin, B. Li, X. Hong, Z. Fan, B. Chen, C. Xue and H. Zhang, Angew. Chem. Int. Ed., 2015, 54, 1210–1214.

[S12] J. Ran, J. Yu and M. Jaroniec, Green Chem., 2011, 13, 2708-2713

[S13] T. Simon, N. Bouchonville, M. J. Berr, A. Vaneski, A. Adrovic, D. Volbers, R. Wyrwich, M. Doblinger, A. S. Susha, A. L. Rogach, F. Jäckel, J. K. Stolarczyk and J. Feldmann, Nature Mater., 2014, 13, 1013-1018.

[S14] H. Yu, X. Huang, P. Wang, J. Yu, J. Phys. Chem. C, 2016, 120, 3722−3730.

[S15] J. Hou, C. Yang, H. Cheng, Z. Wang, S. Jiao, H. Zhu, Phys. Chem. Chem. Phys., 2013, 15, 15660-15668.

[S16] B. Ma, H. Xu, K. Lin, J. Li, H. Zhan, W. Liu, C. Li, Chem. Sus. Chem., 2016, 9, 820–824.

[S17] M. Luo, W. Yao, C. Huang, Q. Wu, Q. Xu, RSC Adv., 2015, 5, 40892–40898.

[S18] Z. Sun, B. Lv, J. Li, M. Xiao, X. Wang, P. Du, J. Mater. Chem. A, 2016, 4, 1598–1602.

[S19] W. Li, S. Xie, M. Li, X. Ouyang, G. Cui, X. Lu, Y. Tong, J. Mater. Chem. A, 2013, 1, 4190–4193.

[S20] K. Chang, Z. Mei, T. Wang, Q. Kang, S. Ouyang, J. Ye, ACS Nano, 2014, 8, 7078−7087.

[S21] H. Katsumata, H. Ando, T. Suzuki, S. Kaneco, Ind. Eng. Chem. Res. 2015, 54, 3532−3535.

[S22] X. Yue, S. Yi, R. Wang, Z. Zhang, S. Qiu, Sci. Rep. 2016, 6, 22268.

[S23] Q. Xiang, F. Cheng, D. Lang, ChemSusChem 2016, 9, 996–1002.

[S24] J. Zhang, Y. Wang, J. Jin, J. Zhang, Z. Lin, F. Huang, J. Yu, ACS Appl. Mater. Interfaces, 2013, 5, 10317−10324.

[S25] C. Wang, L. Wang, J. Jin, J. Liu, Y. Li, M. Wu, L. Chen, B. Wang, X. Yang, B. L. Su, Appl. Catal., B, 2016, 188, 351–359.